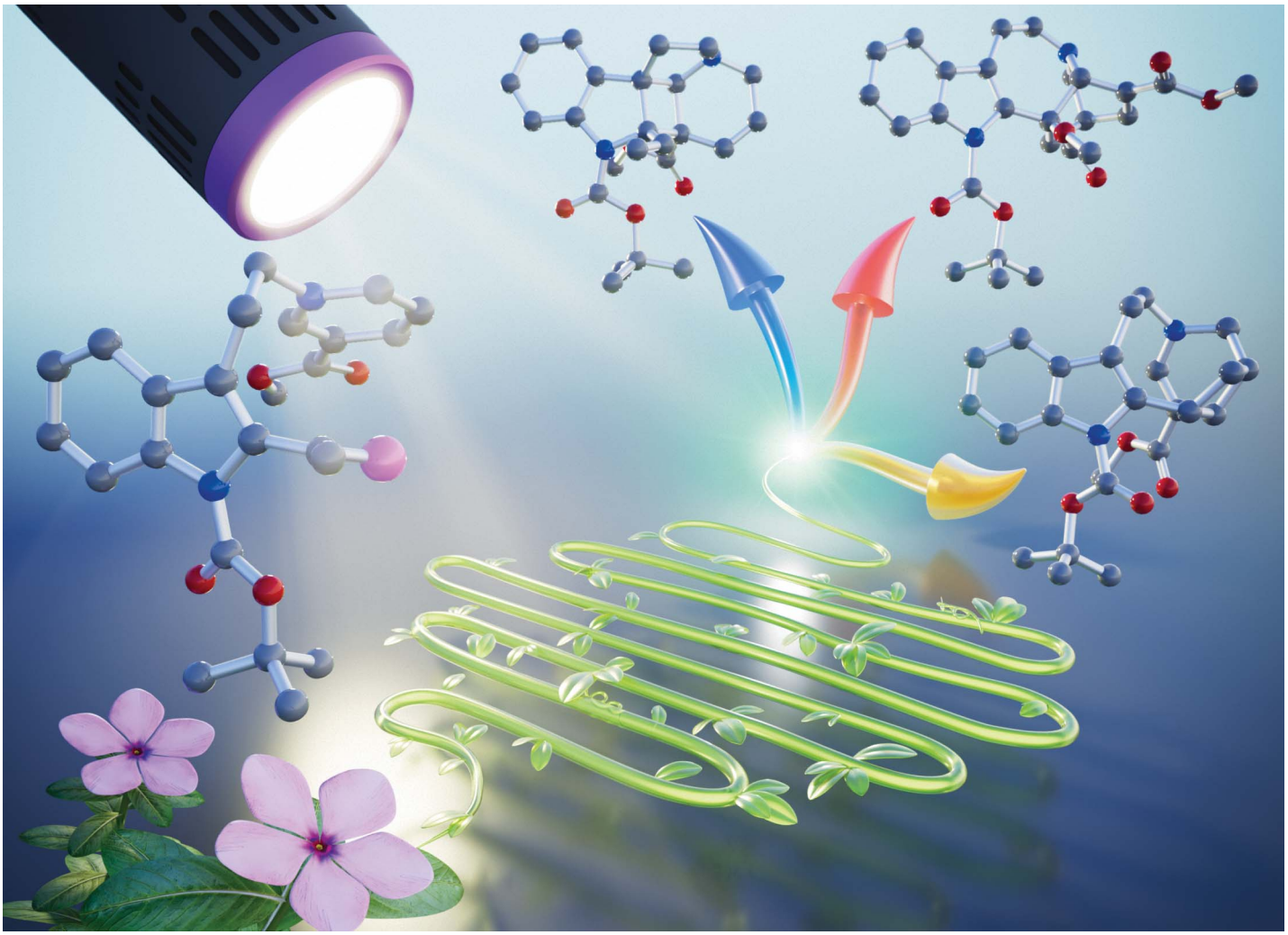

Showcasing research from Professor Hiroki Oguri's laboratory, Department of Chemistry, Graduate School of Science, The University of Tokyo, Tokyo, Japan.

Direct photochemical intramolecular [4+2] cycloadditions of dehydrosecodine-type substrates for the synthesis of the *iboga*-type scaffold and divergent [2+2] cycloadditions employing micro-flow system

A highly efficient, photochemical flow synthesis of three distinct indole alkaloidal scaffolds has been achieved by exploiting conformationally preorganised, multipotent intermediates that closely emulate the plant-derived dehydrosecodine precursor. Through site-selective photoactivation of the dihydropyridine moiety, this strategy unlocks divergent [4+2]/[2+2] cycloaddition pathways, vastly expanding access to complex alkaloidal architectures. Furthermore, it extends natural biosynthetic pathways by harnessing the hidden yet pre-encoded reactivity of the dehydrosecodine-type precursor, eliminating the need for external photocatalysts or photosensitisers.

As featured in:

See Hiroki Oguri *et al.*, *Chem. Sci.*, 2024, **15**, 15599.

ROYAL SOCIETY OF CHEMISTRY

rsc.li/chemical-science

Registered charity number: 207890

Chemical Science

ROYAL SOCIETY OF CHEMISTRY

EDGE ARTICLE

View Article Online
View Journal | View Issue

Cite this: *Chem. Sci.*, 2024, **15**, 15599

All publication charges for this article have been paid for by the Royal Society of Chemistry

Direct photochemical intramolecular [4 + 2] cycloadditions of dehydrosecodine-type substrates for the synthesis of the *iboga*-type scaffold and divergent [2 + 2] cycloadditions employing micro-flow system†

Gavin Tay,‡ Soushi Nishimura‡ and Hiroki Oguri *

Photocyclisation reactions offer a convenient and versatile method for constructing complex polycyclic scaffolds, particularly in the synthesis of natural products. While the [2 + 2] photocycloaddition reaction is well-established and extensively reported, the [4 + 2] counterpart *via* direct photochemical means remains challenging and relatively unexplored. In this work, we devised the rapid assembly of the *iboga*-type scaffold through photochemical intramolecular Diels–Alder reaction using a common biomimetic dehydrosecodine-type intermediate having vinyl indole and dihydropyridine (DHP) sub-units. Exploiting a micro-flow system, the medicinally important *iboga*-type scaffold was obtained up to 77% yield under mild, neutral conditions at room temperature. This study demonstrated the site-selective activation of the DHP moiety by direct UV-LED irradiation, eliminating the need for external photocatalysts or photosensitisers and showing good tolerance to a wide range of stabilised dehydrosecodine-type substrates. By adjusting the spatial arrangement of the DHP ring and the vinyl indole group, this versatile photochemical approach efficiently facilitates both [4 + 2] and [2 + 2] cyclisations, assembling architecturally complex multicyclic scaffolds. Precise photoactivation of the DHP subunit, generating short-lived biradical species, enabled the new way of harnessing the hidden but innately pre-encoded reactivity of the polyunsaturated dehydrosecodine-type intermediate. These photo-mediated [4 + 2] cyclisation and divergent [2 + 2] cycloadditions are distinct from biosynthetic processes, which are mainly mediated through concerted thermal cycloadditions.

Received 19th April 2024
Accepted 15th August 2024

DOI: 10.1039/d4sc02597k

rsc.li/chemical-science

Introduction

Biologically important natural products frequently contain architecturally complex three-dimensional ring systems as intricate components of their core skeletal structure.[1] In particular, the vast majority of these compounds possesses elaborately fused and bridged frameworks, adding an extra layer of complexity to their retrosynthetic analyses and the design of appropriate intermediates for streamlined chemical assembly. Towards this goal, the development of straightforward and flexible synthetic methodologies has become a fundamental objective in organic chemistry. To construct polycyclic rings having a carbon-rich backbone, the classical Diels–Alder (DA) reaction has been extensively employed as a canonical strategy, wherein two unsaturated sub-units, namely the diene and dienophile, undergo a concerted pericyclic annulation to form a new six-membered ring (Fig. 1a).[2] According to the molecular orbital symmetry rules devised by Woodward and Hoffmann in the 1960s,[3] it is well understood that the concerted [4 + 2] cycloaddition process is thermally-allowed in the ground state. While the DA reaction has been proven to be a reliable process, its efficiency and reactivity are greatly dependent on the electronic compatibility between the dienes and dienophiles, constituting a limiting factor in the design of suitable substrates. When this electronic demand is not met, high temperatures are often required to surpass the large activation barrier.

An alternative means by which molecules in the ground state can be activated is with light. Over the last few decades, the application of photochemistry in organic synthesis has grown exponentially and has witnessed remarkable progress in its chemical toolbox.[4] When energy in the form of photons is absorbed, the molecule is elevated to a high-energy excited state. Initiation of the chemical reaction from this vantage point

Department of Chemistry, Graduate School of Science, The University of Tokyo, Hongo, Bunkyo-ku, Tokyo 113-0033, Japan. E-mail: hirokioguri@g.ecc.u-tokyo.ac.jp

† Electronic supplementary information (ESI) available: Synthesis, spectroscopy, crystallography, computational and characterisation details (PDF). CCDC 2333565, 2375152 and 2357172. For ESI and crystallographic data in CIF or other electronic format see DOI: https://doi.org/10.1039/d4sc02597k

‡ These authors contributed equally.

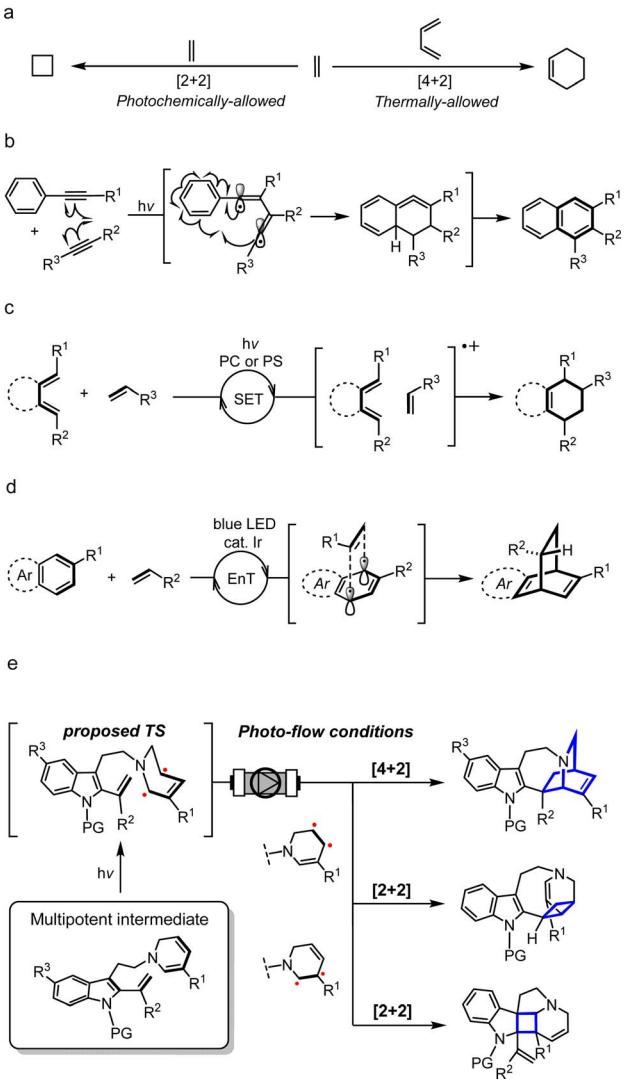

Fig. 1 Scope and chemical space of [4 + 2] cycloaddition reactions. PC: photocatalyst; PS: photosensitizer; SET: single-electron transfer; EnT: energy transfer; TS: transition state.

not only facilitates overcoming high kinetic barriers but can also unveil new and previously inconceivable reaction pathways which are otherwise hidden under thermal conditions. The [2 + 2] cycloaddition to construct a cyclobutane ring is the most ubiquitous and well-known photocycloaddition reaction,[5] and along with numerous other light-driven cycloaddition reactions have provided a straightforward and versatile strategy in organic chemistry for achieving challenging synthetic transformations, particularly the synthesis of natural products.[6]

Since its advent, the scope and chemical space of classical DA reactions have greatly expanded and rapidly advanced into the realm of photochemistry. Early on, it was discovered that the dearomative [4 + 2] cycloaddition of anthracene and maleic anhydride could proceed both thermally and photochemically.[7] Fascinated by the unique reactivities that govern regio- and stereoselectivity, such dearomative DA reactions have been a subject of intense mechanistic investigation. Under thermal conditions, a concerted pathway is widely postulated although some studies have provided evidence for the involvement of biradicals or charge-transfer species depending on the electronic nature of the diene and dienophile.[7a,b] On the contrary, the photochemically-driven process is believed to proceed *via* a biradical mechanism in a stepwise manner, maintaining the orbital symmetry requirements of the Woodward–Hoffmann theory.

Similar to the dearomative DA reaction, dienes in the form of an aryl-alkyne were also found to react under both heat and light.[8] The photochemical process, formerly referred to as the photo-dehydro-Diels–Alder (PDDA) reaction, involves the activation of aryl-alkynes in a triplet excited state, leading to the formation of a C–C single bond with an alkyne as a dienophile, resulting in the generation of a 1,2-butadiene-1,4-diyl biradical intermediate (Fig. 1b). A second C–C bond formation with an aromatic ring generates a strained cyclic allene intermediate, followed by transposition of double bond, which affords a naphthalene ring. Wessig and coworkers recently reported the use of triplet photosensitisers (PSs) such as xanthone to enhance the efficiency of PDDA compared to direct photoirradiation.[8c]

By far the most common strategy for photochemical DA reactions to date is using external photocatalysts (PCs) and PSs, which has seen significant progress since the 1980s (Fig. 1c).[9] Organic photoinduced-electron-transfer (PET) PCs such as pyrylium salts and cyanoaromatic compounds were extensively employed to generate a radical cation as an excited-state intermediate.[9c,d] Triplet ketone PSs including benzoylthiophenes can also induce this transformation *via* triplet state energy-transfer (EnT).[9e,f] On the other hand, Yoon achieved the visible light photocatalysed DA reaction using transition-metal complexes, including Ru and Pt/TiO_2 heterogeneous catalyst, to promote the generation of the radical cation intermediate *via* a photoredox process.[9g–j] More recently, Glorius and Ma developed the metal-catalysed EnT dearomative [4 + 2] cycloaddition of azarenes, predominantly using Ir catalyst under blue LED irradiation (Fig. 1d).[10] On the other hand, several total synthesis routes, including that of estrones[11] and hamigerans,[12] utilised the photoenolisation Diels–Alder (PEDA) reaction as a key strategy to construct the benzannulated cores.[13] UV light activation of the aromatic carbonyl unit triggers *o*-quinodimethane diene formation *in situ*,[14] followed by sequential DA trapping of this intermediate by a dienophile, although the cyclisation step itself is not a photochemically-dependent process.

Nonetheless, DA reactions by direct excitation, particularly towards the biomimetic synthesis of natural products, are still very rare. Herein, we report the photo-induced intramolecular [4 + 2] cycloaddition reaction for the rapid assembly of the bridged [2.2.2]-bicyclic isoquinuclidine ring system of the pharmaceutically intriguing *iboga*-type scaffold from a common dehydrosecodine-type intermediate having 1,6-DHP and vinyl indole moieties as the diene and dienophile, respectively (Fig. 1e). *Iboga*-type mono-terpene indole alkaloids (MIAs) are a significant class of bioactive compounds that possess promising anti-addiction and psychoactive properties.[15] Fascination with this medicinally important family of alkaloids has inspired

the development of numerous synthetic routes, especially towards the construction of the characteristic isoquinuclidine core.[15a] In this novel approach, we utilise direct UV light irradiation to site-selectively photoactivate the 1,6-DHP unit to efficiently promote the formal [4 + 2] cycloaddition. Contrary to common photochemical DA reactions, our strategy does not require the addition of any PCs or PSs. This cyclisation is presumably achieved through stepwise C–C bond formation of transient biradical intermediates. Importantly, the application of a micro-flow system facilitated streamlined assembly of the pentacyclic scaffold of *iboga*-type MIAs in modest to high yields under mild reaction conditions at room temperature, with short irradiation times through enhancing the photoirradiation efficiency while minimising decomposition. Furthermore, removal of the methyl ester moiety at the vinyl indole unit induced subtle but significant changes in the pre-organised conformation of the stabilised dehydrosecodine-type intermediate, paving the way for the divergent photo-mediated [2 + 2] cyclisations. These intricate and topologically complex multicyclic scaffolds are inaccessible through the enzymatic conversions and biomimetic synthesis relying on the thermal concerted cycloadditions.

Results and discussion

Synthesis of intermediate and its biomimetic thermal DA reaction leading to *iboga*-type scaffold

Azepinoindole intermediate **1a** was prepared from tryptamine hydrochloride through the modular assembly of three building blocks in four steps, which included a Pictet–Spengler cyclisation, ring expansion, reduction, and *N*-propargylation (Fig. 2). In a previous study, we reported the biogenetically-inspired synthesis of *iboga*/*aspidosperma*-type alkaloidal scaffolds, utilising a common multipotent intermediate **3a** that possesses both vinyl indole and 1,6-DHP moieties.[16] This intermediate **3a**, designed to mimic and preserve the structural features of dehydrosecodine **4**, only differs by installing an electron-withdrawing ester group at the C3 position of the labile DHP ring in place of the ethyl substituent for improved stability through modulation of its electron density. Under microwave-assisted heating at 60 °C, Cu(I)-catalysed *in situ* 6-*endo* cyclisation of the 1,6-DHP ring (**2a** → **3a**)[17] and subsequent intramolecular biomimetic DA cycloaddition proceeded to give the *iboga*-type scaffold **5a** in 48% yield (two steps).

A notable drawback of our previously designed synthetic process has been the instability of the indole-free ene-yne precursor **2a**, without protection of the indole, which is prone to gradual decomposition by intra- and intermolecular Michael additions.[16] To stabilise this precursor, and ease its handling, we installed an electron-withdrawing 2-(trimethylsilyl)ethoxycarbonyl (Teoc) carbamate protecting group at the indole N1 position of **1a** to give **1b**. Then, treatment with methyl propiolate triggered a tandem one-pot transformation involving hetero-Michael addition and Hofmann elimination to afford the stable indole-protected ene-yne **2b** in almost quantitative yield. Cu(I)-catalysed conversion of **2b** generated the dehydrosecodine-type intermediate **3b** with efficient formation of the 1,6-DHP ring. However, subsequent one-pot DA cycloaddition with microwave-assisted heating to yield the corresponding *iboga*-product **5b** did not proceed at all. Raising the temperature to 80 °C only led to gradual isomerisation of the 1,6-DHP unit in **3b** to the 1,4-DHP. Regarding the biomimetic dehydrosecodine-type intermediate **3a**, it is believed that the contribution of hydrogen bonding interactions between the free indole NH and neighbouring methyl ester unit plays a crucial role in increasing the electrophilicity of the dienophile, as well as achieving precise conformational pre-organisation suitable for the concerted DA reaction.[16]

Photochemical [4 + 2] cycloaddition to assemble *iboga*-type scaffold

With this in mind, we instead envisioned the construction of the isoquinuclidine [2.2.2]-bicyclic bridged ring system of the

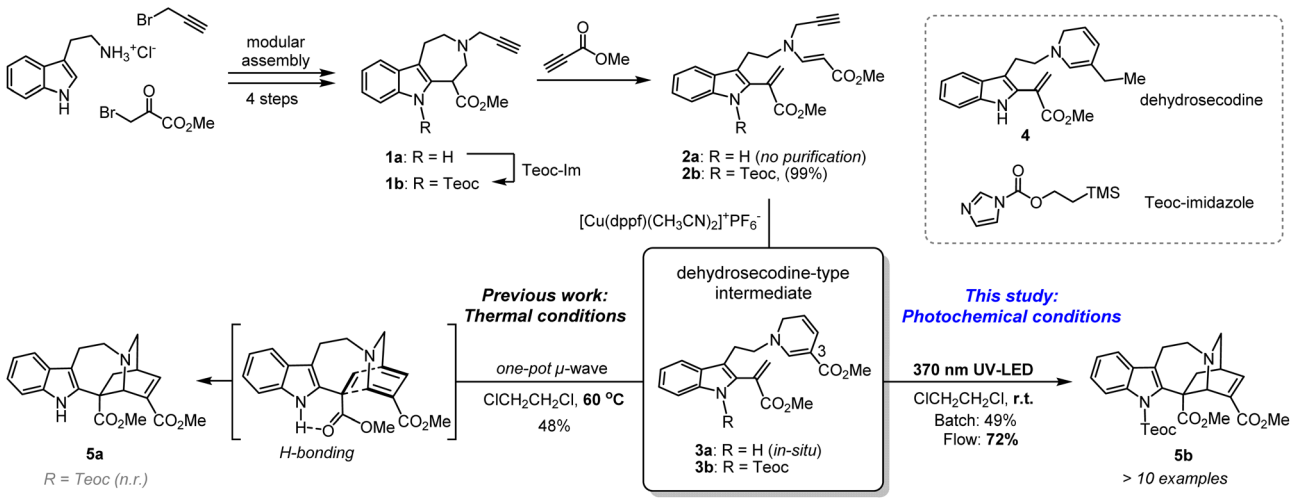

Fig. 2 Synthesis of common biomimetic dehydrosecodine-type intermediates 3 and *iboga*-type scaffolds 5 *via* thermal and photochemical pathways.

iboga-type skeleton by photochemical means. Preliminary UV-Vis analysis of the dehydrosecodine-type intermediate **3b** showed a strong UV absorption peak at 356 nm ($\varepsilon = 6.16 \times 10^3$ M^{-1} cm^{-1}) in $CHCl_3$ (Fig. S9†). Based on the absorption wavelength of the intermediate **3b**, we attempted the photoreaction using a 370 nm UV-LED lamp (30 W). Cu(I)-catalysed 6-*endo* cyclisation of the Teoc-protected ene-yne precursor **2b** in degassed 1,2-dichloroethane formed the 1,6-DHP ring. To our delight, subsequent irradiation for 4 h successfully furnished the corresponding *iboga*-product **5b** with formation of a quaternary carbon centre, albeit in low yield of 30% over two steps (see Table S1†). Taking this finding as a starting point, we commenced the systematic optimisation of photoreaction conditions under batch conditions (Table 1). Upon photoirradiation of **2b** in 1,2-dichloroethane as the solvent, we found that 90 min was the optimal reaction time. This condition afforded the product **5b** in 42% yield (41% isolated yield) based on NMR analysis using an internal standard (entry 1). Prolonged exposure of the reaction solution to UV light irradiation potentially led to the decomposition of the product, although such byproducts could not be isolated or identified. A survey of various solvents suggested that toluene was the ideal choice (entries 1–4), and irradiation at 370 nm gave the best results (entries 5–7), consistent with the UV-vis spectrum (Fig. S9†). When we changed the bidentate phosphine ligand for the Cu(I) catalyst from 4,5-bis(diphenylphosphino)-9,9-dimethylxanthene (Xantphos) (**6**) to 1,1′-bis(diphenylphosphino)ferrocene (DPPF) (**7**), the yield for the two-step sequential conversion (**2b** → **3b** → **5b**) improved to 55% (49% isolated yield) (entry 8).

Table 1 Optimisation of photoreaction under batch conditions

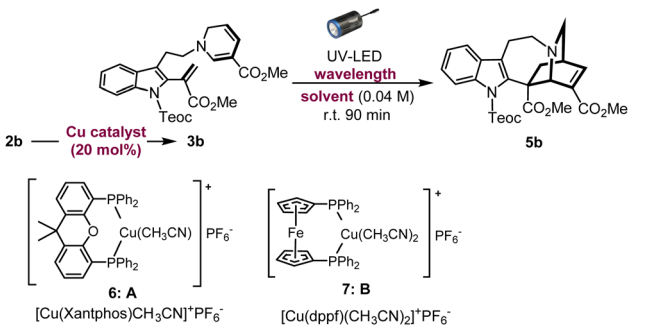

Entry	Solvent	Catalyst	Wavelength	Yield of **5b**[a]
1	$ClCH_2CH_2Cl$	**A**	370 nm	42% (41%)[c]
2	MeCN	**A**	370 nm	27%
3	Toluene	**A**	370 nm	43%
4	Benzene	**A**	370 nm	41%
5[b]	Toluene	**A**	280 nm	4%
6	Toluene	**A**	427 nm	30%
7	Toluene	**A**	456 nm	Trace
8	**Toluene**	**B**	**370 nm**	**55% (49%)**[c]

[a] Yield of **5b** was determined as a two-step yield by ^1H NMR spectroscopic analyses using triphenylmethane as an internal standard. [b] Reaction mixture was irradiated for 3 h. [c] Isolated yield over two steps. Xantphos = 4,5-bis(diphenylphosphino)-9,9-dimethylxanthene; DPPF = 1,1′-bis(diphenylphosphino)ferrocene.

Substantial improvement using micro-flow system

In an effort to enhance the completion of the photoreaction, we conceived of employing the micro-flow system to simultaneously increase the photoirradiation efficiency and control the exposure time of the reaction solution under UV light, thereby suppressing the overreaction of the resulting *iboga*-product **5b**. Recently, the application of photo-flow technology in synthetic organic chemistry, both in the laboratory and industrial settings, is rapidly expanding due to its improved reaction efficiency, ease of scalability, as well as practical cost and environmental benefits.[18] Unlike thermal batch conditions, whereby the temperature within the reaction vessel remains uniform, photochemical reactions are highly sensitive to distance between the light source and reaction media owing to the rapid attenuation of light intensity. By employing the micro-flow chamber as the reaction vessel, we can achieve a more uniform irradiation and significantly reduce the distance that light needs to penetrate through the solvent media to enhance the overall irradiation efficiency. Under flow conditions, diluting the reaction concentration from 0.04 M to 0.01 M led to a substantial increase in yield, reaching 61% (51% isolated yield) with an optimal reaction time of just 25 min (Table 2: entries 1–6). However, the slight insolubility of intermediate **3b** in toluene, the ideal solvent under batch conditions, caused gradual precipitation inside the flow chamber. Consequently, changing the solvent to 1,2-dichloroethane considerably improved the yield, affording the *iboga*-product in 74% (72% isolated yield) from **2b** over two steps (entry 7). When the reaction scale was increased by six-fold, the *iboga*-product **5b** (213 mg, see Page S28† for details) was still obtained in 68% yield.

Table 2 Optimisation of photoreaction under flow conditions

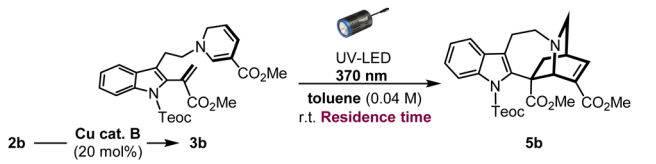

Entry	Deviation from batch	Residence time	Yield of **5b**[a]
1	None	15 min	24%
2	None	20 min	41%
3	None	25 min	35%
4	0.01 M	15 min	53%
5	0.01 M	20 min	55%
6	0.01 M	25 min	61% (51%)[b]
7	0.01 M $ClCH_2CH_2Cl$	25 min	74% (72%)[b]

[a] Yield of **5b** was determined as a two-step yield by ^1H NMR spectroscopic analyses using triphenylmethane as an internal standard. [b] Isolated yield over two steps. Cu cat. **B** = $[Cu(dppf)(CH_3CN_2)]^+PF_6^-$.

Substrate scope and limitation

Using the optimised photoreaction conditions, we aimed to explore the general applicability of the formal [4 + 2] cycloaddition through substrate scope expansion (Fig. 3). Firstly, all tested substituents on the indole nitrogen, including carbamate, methyl, and benzyl groups, were well tolerated for this photo-[4 + 2]-cycloaddition. Among the five substrates, **3b–3f**, protection with an electron-withdrawing carbamate group at the indole N1 led to efficient conversions, and the best result was achieved with the cycloaddition of **3d** with a methyl carbamate protection to furnish corresponding *iboga*-type scaffold **5d** in high yield of 77%. Meanwhile, substrates **3e** and **3f** having an electron-donating substituent at the indole N1 resulted in slower reactions, potentially due to an electronic mismatch between the reacting sub-units, although the photoreaction still proceeded modestly. Next, the substrate scope for the DHP ring was examined. Installation of electron-withdrawing groups in the substrates (**3g–h**, and **3m**) at the C3 position of the DHP ring yielded mixed results. Substrates **3g** and **3h**, bearing sulfonyl and ketone moiety, respectively, provided good yields of the corresponding [4 + 2] cycloadducts, **5g** and **5h**,[19] comparable to their methyl ester counterpart **5b**. However, substrate **3i** with an aldehyde group instead resulted in a significantly slower reaction, presumably attributed to its excessively strong electron-withdrawing nature. Meanwhile, an attempted conversion of substrate **3j** bearing an amide group did not yield the corresponding product **5j** at all. We presume that the weakly electron-withdrawing amide group was insufficient to adequately stabilise the oxidation-labile 1,6-DHP unit, potentially causing an undesired hydride shift from the C6 position and rapid decomposition into the pyridinium species. The negligible differences in both the molar absorption coefficient and spectral profiles among the UV-vis spectra in $CHCl_3$ for **3b** ($\varepsilon = 6.16 \times 10^3\ M^{-1}\ cm^{-1}$), **3e** ($\varepsilon = 6.32 \times 10^3\ M^{-1}\ cm^{-1}$) (Fig. S10†), and **3i** ($\varepsilon = 6.31 \times 10^3\ M^{-1}\ cm^{-1}$) (Fig. S11†) strongly suggest that there is essentially no decrease in the light absorption efficiency between the substrates, despite the lower yields observed for *iboga*-type products such as **5e** and **5i**.

Subsequently, to assess the necessity of the ester group at the vinyl indole position, we attempted to replace it with a phenyl group *via* Au(I)-catalysed alkenylation[20] of the indole C2 position, with substrate **3m** having a *N*-Boc carbamate protecting group at the indole (for synthesis scheme, see Pages S13–S16†). However, the resulting photo-mediated [4 + 2] cyclisation of **3m** to **5m** failed to proceed, likely due to the steric hindrance near the phenyl group.

Divergent [2 + 2] cycloadditions

As an attempt to reduce the steric hindrance in **3m**, we then prepared substrate **3n** with removal of the phenyl group at the vinyl indole unit (for synthesis scheme, see Pages S16–S19†). The photoirradiation of **3n** under micro-flow conditions led to distinct and notable results (Fig. 4a and see Page S30† for details). Unlike the attempt with substrate **3c** bearing a methyl ester moiety, the formation of the *iboga*-type scaffold was turned to be substantially diminished and resulted in **5n** in a minute amount with the yield of 9%. More importantly, we unexpectedly encountered divergent [2 + 2] cyclisations to two distinct scaffolds in combined yield of 87%. The subtle structural

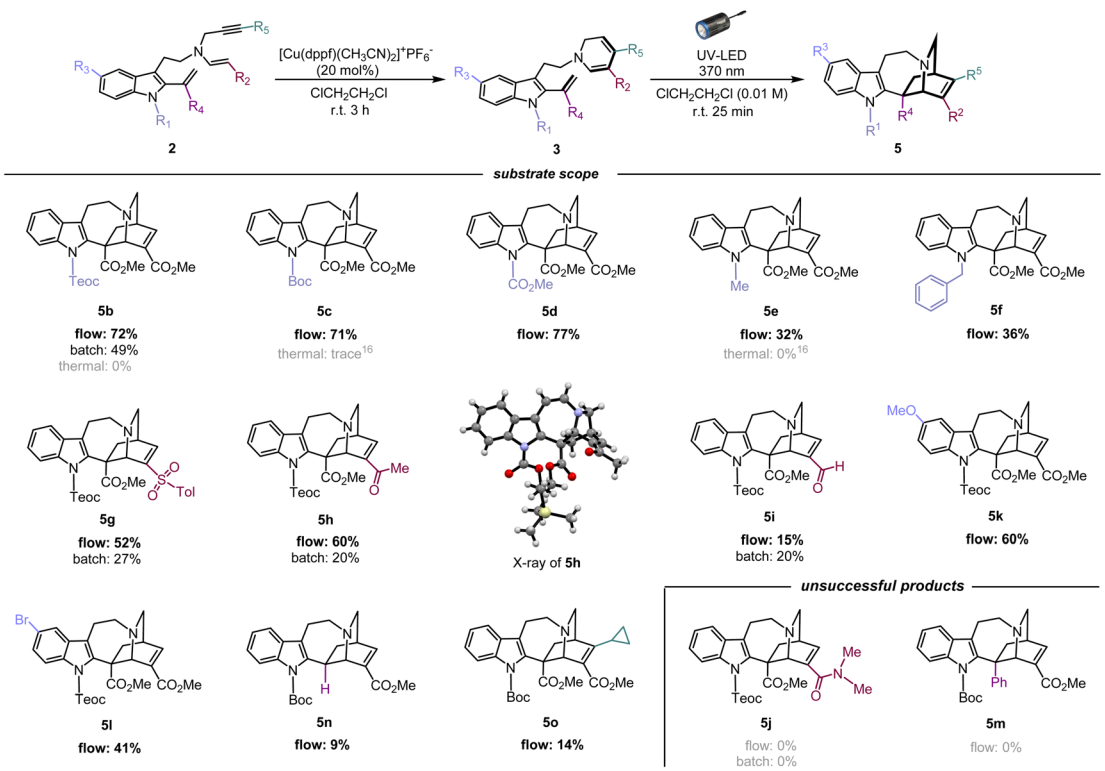

Fig. 3 Substrate scope and limitations of [4 + 2] photocycloaddition for assembly of the *iboga*-type product.

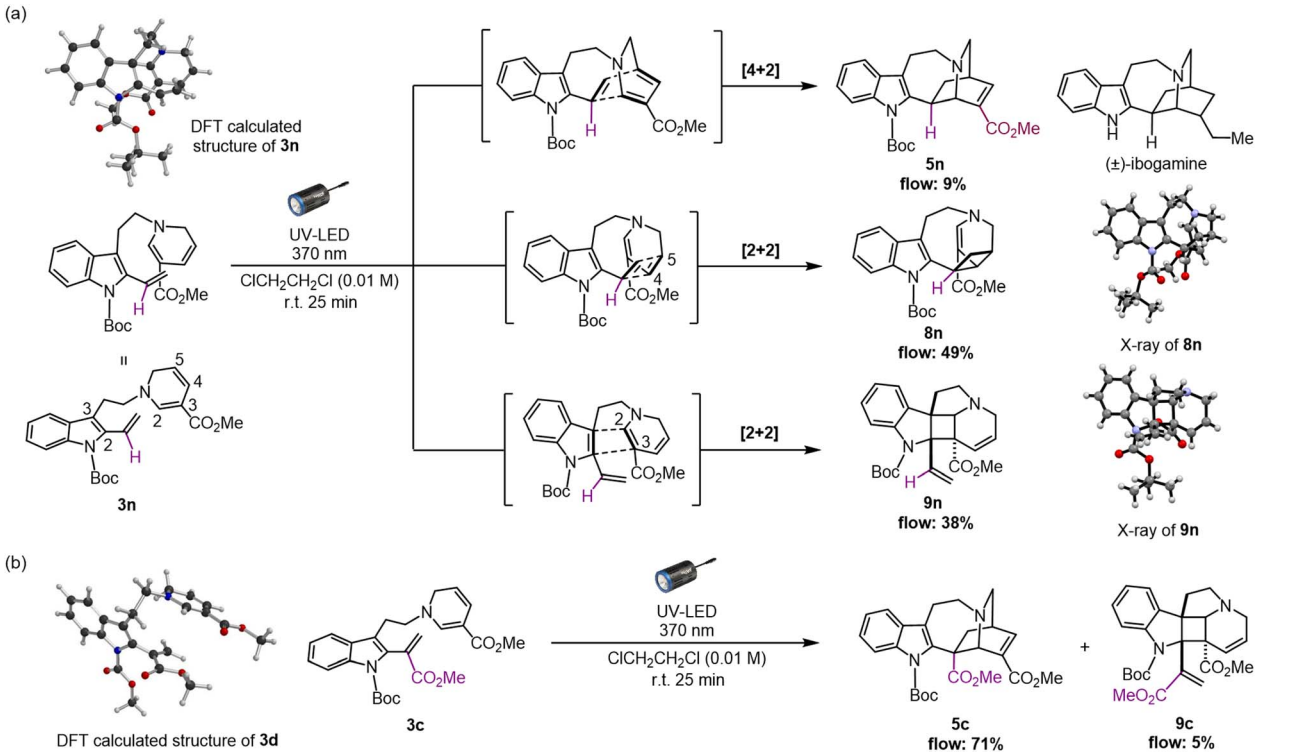

Fig. 4 (a) Unexpected divergent [4 + 2] and [2 + 2] cycloadditions of **3n** to form *iboga*-type scaffold **5n**, and novel indole alkaloidal scaffolds **8n** and **9n**, respectively. (b) Re-analysis of photoreaction from **3c**. DFT modelling of **3d** and **3n** were performed using the B3LYP-D3 (6-31+G*) level of theory.

change, the removal of the methyl ester group in precursor **3n**, induced a drastic alteration of the intramolecular cyclisation mode. The major product **8n** was assembled in 49% yield *via* a [2 + 2] cycloaddition between the vinyl indole and the C4–C5 olefinic double bond of the 1,6-DHP.[19] In addition, a dearomative [2 + 2] cycloaddition between the indole C2–C3 double bond and an olefin at the C2–C3 position of the 1,6-DHP also proceeded to form pentacyclic spiroindoline scaffold **9n** in 38% yield. This photo-mediated dearomative [2 + 2] cyclisation enabled the diastereo-controlled formation of the three consecutive quaternary carbon centres within the central cyclobutane framework in **9n**.[19] In fact, the relevant intra- and intermolecular [2 + 2] cycloaddition reactions with the indole ring have been reported using blue-LED or visible light in the presence of PCs.[21] We postulate that the absence of any substituent at the vinyl indole unit induces a slight conformational shift in the spatial arrangement of the reacting sub-units, sufficient to favour the [2 + 2] cycloaddition while severely inhibiting the [4 + 2] cyclisation reaction pathway.

To confirm the possibility that the [2 + 2] cycloadditions compete with the photo-mediated [4 + 2] cyclisation, even in trace amounts, we carefully re-analysed the photochemical reaction using **3c** as a representative substrate for the high-yield formation of the *iboga*-type scaffold **5c** (Fig. 4b). Indeed, the formation of **9c** through the corresponding dearomative [2 + 2] cycloaddition was observed, albeit with a very low yield of 5%. Meanwhile, the occurrence of the other [2 + 2] cycloaddition leading to scaffold **8c** was not detected at all.

In our recent study, we successfully elucidated the X-ray crystallographic structure of unstable dehydrosecodine-type intermediate **3** through host-guest encapsulation within a self-assembled coordination cage.[22] The resulting X-ray analysis of guest molecule **3d** revealed the unique stacking of both reacting sub-units, the 1,6-DHP ring and vinyl indole moiety, conformationally primed to undergo the [4 + 2] cycloaddition. This finding was consistent with DFT computational modelling (Fig. S7†).[23] Notably, the energy minimised structure of **3n** (Fig. S8†) revealed an adopted conformation with the folding of the DHP ring towards the indole ring and evidently aligning the four reacting olefins, representing a pre-organised spatial arrangement that favours the [2 + 2] cycloadditions over the corresponding [4 + 2] annulation. Thus, the methyl ester group in the vinyl indole moiety of **3c** appears to possess the "Goldilocks effect" as a precise steric handle that selectively facilitates the assembly of the *iboga*-type scaffold **5c**. To the best of our knowledge, the [2 + 2] cycloadducts **8** and **9** are novel, bis-nitrogen containing, densely functionalised sp^3-rich scaffolds relevant to MIAs. These unnatural intricate alkaloidal scaffolds are inaccessible under previous thermal conditions or by chemoenzymatic means.

Mechanistic studies

We then turned our attention to elucidating the photoreaction mechanism (Fig. 5, see the ESI† for details). To probe the origin of the characteristic UV absorption at approximately 356 nm for **3b**, we first conducted regio-selective hydrogenation of the C4–

C5 double bond of the 1,6-DHP unit to generate the stable tetrahydropyridine (THP) product **10** (Fig. 5a).[16] After reduction, no UV absorption was observed at this wavelength, indicating that the 356 nm absorption is derived from the conjugated system of the 1,6-DHP ring. This also strongly suggests that direct irradiation induces site-selective activation of the DHP moiety to trigger the [4 + 2] cyclisation.

To investigate whether an electron donor–acceptor (EDA) pair could form between the electron-rich DHP and electron-deficient vinyl indole moieties upon photoexcitation,[24] we prepared a pair of model substrates, vinyl indole **11** and 1,6-DHP **12**,[16,22,25] and verified the possibility of their complexation through UV-vis analysis in $CHCl_3$ (Fig. 5b). However, no significant shifts in the absorption spectrum were observed, indicating that an EDA pair is not likely to be involved in this system. The absence of solvent-dependent spectral shifts of the cyclisation precursor **3b**, as the stabilised dehydrosecodine-type substrate, also supports this result (Fig. S15†).

We then wondered whether the Cu(I) catalyst, utilised in the initial step to form the 1,6-DHP ring (**2b** → **3b**), could act as a PC to facilitate the photoreaction. DA reactions promoted by copper salts have been extensively reported, and are particularly useful for hetero-DA reactions, as well as for enantioselective synthesis by employing chiral copper complexes.[26] After cyclisation of the DHP ring, commercially available metal scavenger, SiliaMetS Diamine (10.0 equiv. to Cu) was added and then stirred for 1 h (Fig. 5c). Successful complexation of the scavenger with Cu(I) was confirmed by a visible change to a blue colour of the silica support, which was subsequently removed by filtration through a short pad of silica. When the resulting solution was subjected to photoreaction under standard flow conditions, the *iboga*-scaffold **5b** was still obtained in 65% yield. The slight decrease in yield could be attributed to the additional manipulation of the labile intermediate **3b**. Furthermore, the Cu(I) catalyst $[Cu(dppf)(MeCN)_2]^+PF_6^-$ (7) itself does not show UV absorption at around 370 nm (Fig. S16†). These experimental results have confirmed that the light-mediated [4 + 2] intramolecular cyclisations proceeds without the need for the copper complex to act as a photocatalyst.

At this point, we anticipated that the photo-mediated [4 + 2] cycloaddition of **3b** proceeds *via* a series of transient biradical intermediates upon photoactivation of the 1,6-DHP unit. To attest our hypothesis, we attempted radical trapping under flow conditions using (2,2,6,6-tetramethyl-1-piperidinyloxyl) (TEMPO) radical, 1,1-diphenylethylene, and butylated hydroxytoluene (BHT) (Fig. 5d). In the presence of the radical trapping agents (10 equiv.), the yield of *iboga*-product **5b** decreased by approximately half (Table 3). LCMS-IT-TOF analysis indeed revealed formation of the corresponding adduct bearing two additional hydrogens donated from BHT (Fig. S17†) as well as a 1 : 1 adduct with 1,1-diphenylethylene (Fig. S18†), although isolation of these products to deduce their exact structures was not possible. It is likely that the competing intramolecular cyclisation occurred very rapidly, therefore the formation of the

Table 3 Radical trapping experiments

Entry	Radical trapping agent	Yield of **5b**
1	2,2,6,6-Tetramethylpiperidinyloxyl (TEMPO) radical	38%
2	Butylated hydroxytoluene (BHT)	34%
3	1,1′-Diphenylethylene	40%

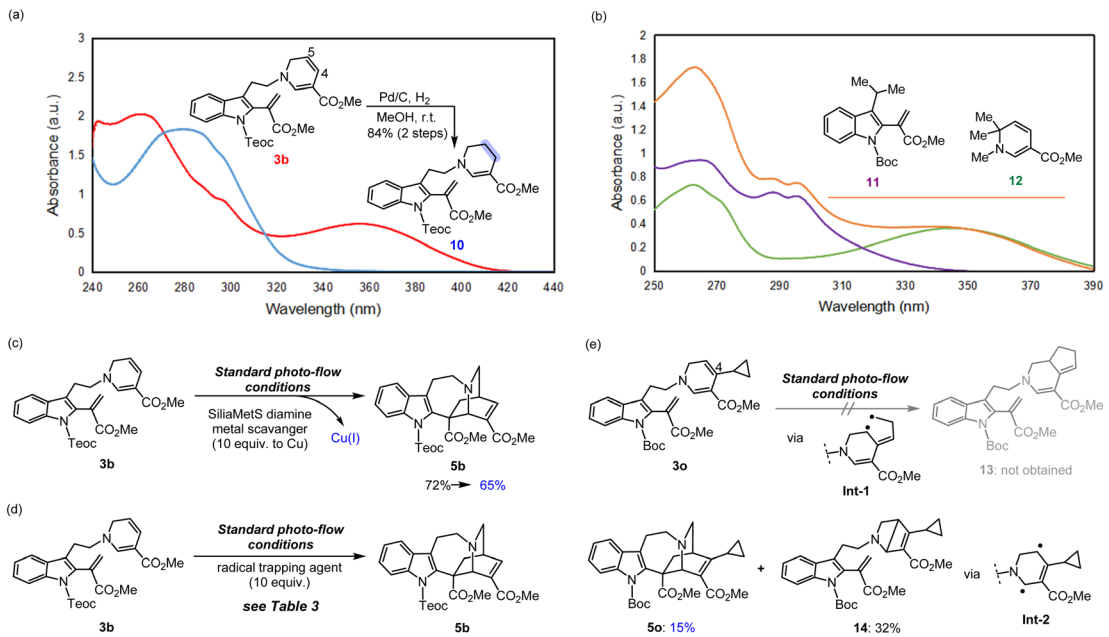

Fig. 5 Mechanistic studies of [4 + 2] cycloaddition. (a) UV-vis spectral analysis of DHP intermediate **3b** and THP **10** in $CHCl_3$. (b) UV-vis spectral analysis of EDA complex *via* model substrates **11** and **12** in CHCl. (c) Photoreaction under Cu(I)-free conditions. (d) Radical trapping experiments. (e) Radical clock experiment.

iboga-product **5b** could not be sufficiently prevented even when excessive quantities of the radical trapping agents were added.

Next, we designed and synthesised radical clock substrate **3o**, by incorporating a cyclopropane moiety at the C4 position of the DHP ring (Fig. 5e). To attain **3o**, the cyclopropane unit was pre-installed to the propargyl bromide fragment prior to *N*-propargylation (for synthesis scheme, see Pages S19 and S20†). Upon the photo-mediated generation of biradicals from the radical clock substrate **3o**, we anticipated a sequential radical-mediated cyclopropane ring opening to generate intermediate **Int-1**, followed by the formation of a five-membered ring leading to **13**. However, contrary to our expectations, products like **13** were not observed while the *iboga*-scaffold **5o** still formed, albeit in a low yield of 15%. Unexpectedly, the formation of a nitrogen-containing bicyclo[2.2.0] ring system, presumably through **Int-2**, predominantly occurred to produce **14** in 32% yield as the major product. These experimental findings are consistent with our previous results, where photoexcitation of the 1,6-DHP ring leads to the generation of biradical species. The 4π-electrocyclic ring-contraction of relatively electron-rich DHPs, pyridones, and other conjugated cyclic systems has been reported to occur under UV light irradiation *via* the singlet excited state.[27] The electron density of the DHP moiety likely increased due to inductive effects from the introduction of the electron-donating cyclopropane moiety into the electron-deficient DHP ring bearing the methyl ester substituent. This change in electronic properties probably facilitated the 4π-electrocyclisation of **3o** to **14**, a reaction otherwise not observed in the photochemical cycloadditions of substrates **3b–n** without the cyclopropane substituent on the DHP ring.

A plausible reaction mechanism

Based on a series of spectral analyses, experimental outcomes, as well as accumulated circumstantial evidence, we propose a stepwise biradical mechanism for the [4 + 2] cyclisation reaction (Fig. 6). Upon UV light irradiation, the 1,6-DHP moiety of **3** undergoes photochemical excitation to reach a high energy excited state, leading to the formation of interconvertible biradical intermediates denoted as **Int-A**. Among the three biradicals in equilibrium, **Int-A2**, having the biradicals at the DHP C2 and C5 positions, is expected to have the highest spin density, as evidenced by the formation of the bicyclo[2.2.0] ring (**3o** → **14**). From **Int-A2**, two distinct radical reaction pathways to form a C–C bond can be conceived. It is likely that pathway **B** is favoured over pathway **A**, since pathway **A** generates a biradical intermediate **Int-B** which contains a highly unstable primary radical. In contrast, pathway **B** forms a corresponding intermediate **Int-C** capable of stabilising the resulting radical through conjugation with the indole ring on the left. Subsequent radical coupling from this stabilised intermediate **Int-C** would furnish *iboga*-scaffold **5**.

In a similar manner, we postulate the divergent intramolecular [2 + 2] annulations of **3** to assemble **8** and **9** could also proceed from the same excited state intermediate **Int-A** (Fig. 6). UV-vis analysis (Fig. S12†) revealed that there is negligible red-shift in the absorption spectrum of the conjugated vinyl indole moiety in substrate **3n** compared to **3b**. These experimental findings strongly suggest that the [2 + 2] cycloadditions are also initiated through the direct photoactivation of the 1,6-DHP ring rather than the vinyl indole. Thus, **Int-A1** and **Int-A3** could directly and rapidly give rise to scaffolds **8** and **9**, respectively, with exquisite control of diastereoselectivity. The retro-[2 + 2] reactions of the cycloadducts **8** and **9** do not occur at all under 370 nm light irradiation at room temperature, strongly indicating that there is no photo-reversible interconversion among the three scaffolds **8**, **9**, and **5** under the reaction conditions. Importantly, the ability to induce C–C bond formation at all four olefinic centres on the 1,6-DHP ring (C2 to C5) also confirms the presence of transient resonance stabilised biradical species **Int-A1** to **Int-A3**. It is worth noting that unlike previously reported [2 + 2] cycloadditions with the indole C2–C3 double bond, our photochemical cyclisation does not rely on the use of external PCs or PSs to generate the cyclobutane-fused indoline-type products **9**.[21] As revealed by DFT computational modelling of **3n**, the challenging dearomative transformation (**3** → **9**) could be facilitated by the inherent pre-organisation of the two reacting olefinic double bonds. The novelty of this finding thus holds considerable significance as a direct and feasible approach to access such fused heterocyclic spiroindoline scaffolds.

Through our investigations, we have showcased the efficiency and adaptability of a biogenetically-inspired approach that flexibly accesses diverse indole alkaloidal scaffolds from the common stabilised multipotent intermediates **3**, mimicking dehydrosecodine (**4**), which is biosynthetically derived from tryptamine and secologanin (Fig. 7).[16] The synthetically tractable indole-free analogue **3a** has paved the way to the biomimetic assembly of *iboga*-type alkaloid **5a**, aided by hydrogen-bonding-mediated conformational pre-organisation and heating. Yet, because of its high reactivity, the utility of **3a** has been severely restricted to an *in situ* generated species. Such labile intermediates bearing multiple sensitive structural components are highly susceptible to unwanted side-reactions under heat due to unpredictable conformational changes and uncontrollable activation of reactive sites. Moreover, efforts to further stabilise **3a** *via* protection of the indole N1 position was ultimately met with a complete loss of desirable reactivity, even under harsher thermal conditions. Using this newly developed photo-mediated strategy, we were able to successfully circumvent these synthetic complications and shortcomings. Despite the dormancy of indole-protected substrates like **3b** towards thermal-mediated DA cyclisations, its inherent reactivity can be efficiently triggered by site-selective photochemical excitation of the DHP unit. The simple modification of the substituent on the vinyl indole moiety in the substrate **3n** revealed the remarkable efficiency of the [2 + 2] cycloaddition reactions. This enables the divergent synthesis of the pentacyclic scaffolds **8n** and **9n** with high cumulative yield and excellent regio- and diastereoselectivity in the formation of the densely functionalised central cyclobutane ring. Yet, by leveraging the exquisite conformational control afforded by the methyl ester substituent on the vinyl indole moiety, we circumvented these rapid and photochemically-intrinsic [2 + 2] cycloadditions. Instead, we

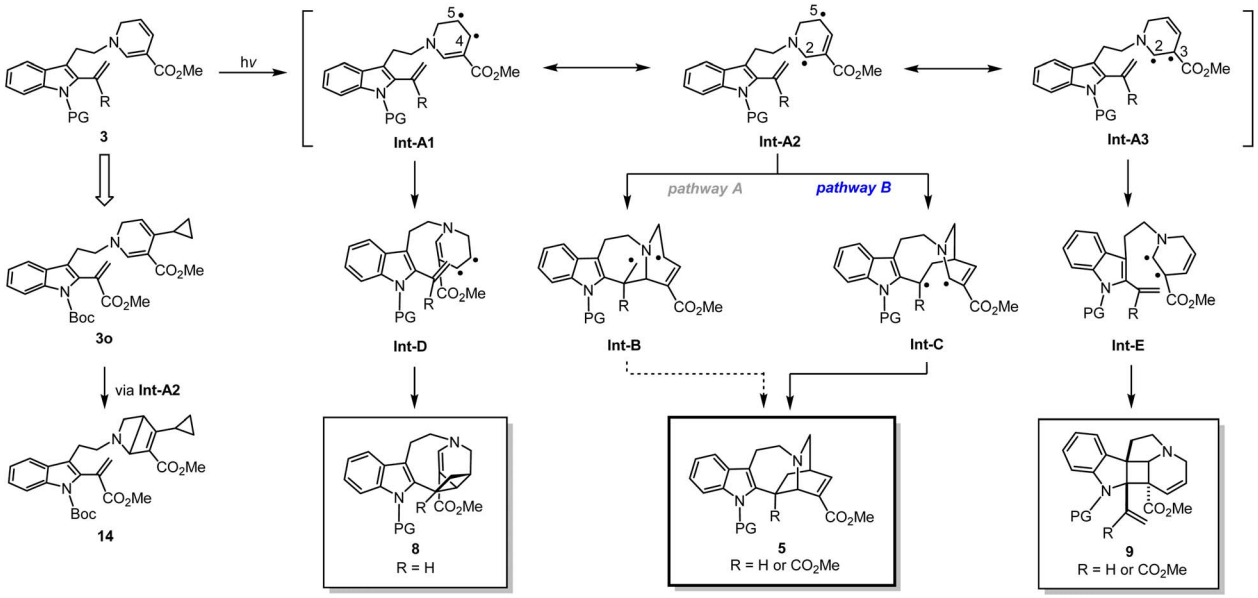

Fig. 6 Proposed reaction mechanism of formal [4 + 2] and [2 + 2] cycloadditions *via* a biradical pathway.

successfully engaged in the more challenging and less common photo-mediated [4 + 2] cyclisation, leading to the *iboga*-type scaffold through a stepwise reaction pathway involving a series of reactive biradical intermediates. This unique feature of our study is distinctly defined by the precise light activation and the preservation of the innate proximity of the reaction sites with minimal conformational changes, as demonstrated with substrates **3c** and **3n**. Hence, we have unveiled a novel synthetic utility for multipotent intermediates **3b–n**, which possesses the dehydrosecodine-type polyunsaturated system. These versatile yet stabilised and manipulable intermediates enable the efficient and precise construction of intricately fused and densely functionalised scaffolds under mild, neutral photochemical conditions otherwise unattainable by thermal processes.

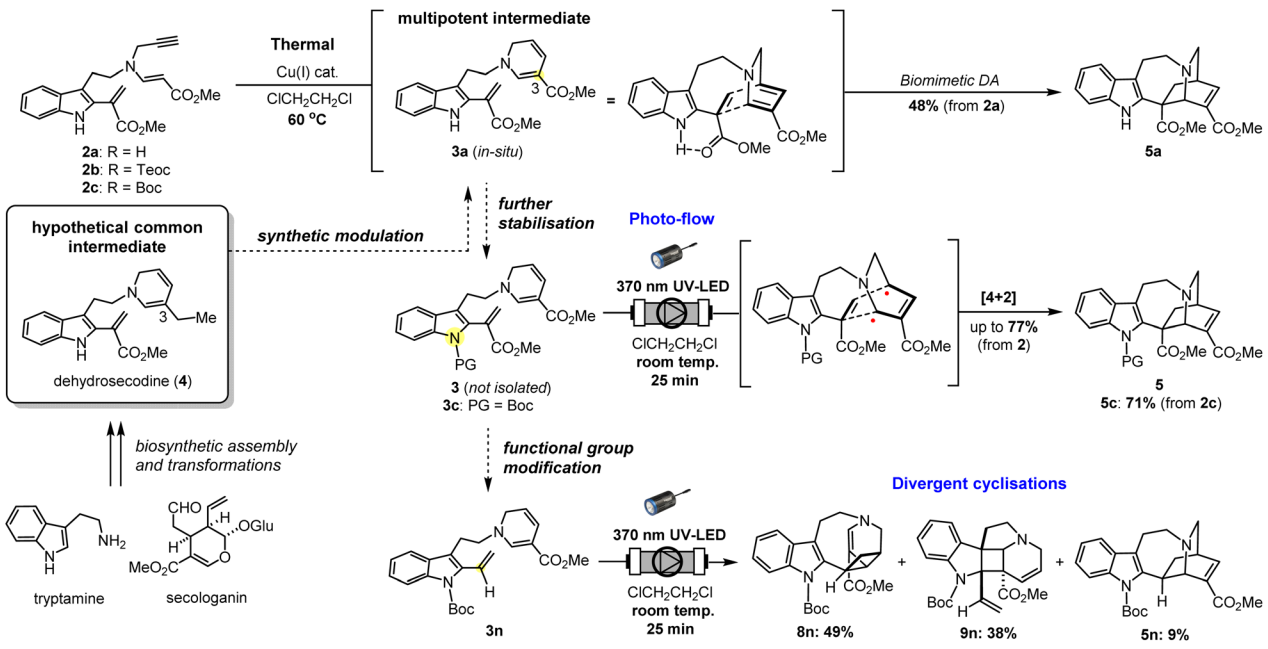

Fig. 7 Biosynthesis of dehydrosecodine (**4**) initiates from tryptamine and secologanin as building blocks. The thermal biomimetic [4 + 2] cycloaddition proceeds *via* a dehydrosecodine-type multipotent intermediate (**3a** → **5a**) facilitated by both heating and an intramolecular hydrogen-bonding. The new photo-flow approach features site-selective activation of DHP moiety using stabilised substrates **3** with indole N1 protection. A biradical reaction pathway enabled the divergent [4 + 2] and [2 + 2] cyclisations with minimal conformational changes in the pre-organised structures of **3c** and **3n**, respectively.

Conclusions

In conclusion, we achieved the direct and additive-free photochemical [4 + 2] cycloaddition reaction to efficiently assemble the bridged [2.2.2]-bicyclic isoquinuclidine ring system of the *iboga*-type scaffold. The introduction of an indole N1 protecting group substantially stabilised the ene-yne precursors **3** for ease of handling and storage. Simultaneous implementation of micro-flow conditions to our reaction system was crucial to substantially enhance the photoirradiation efficiency while taming unwanted overreactions arising from overexposure to UV light under traditional batch methods. Compared to previously reported thermal conditions, our facile and scalable photochemical approach showed excellent tolerance to a diverse range of substrates in modest to high yields. Mechanistic studies strongly suggest the generation of biradical species upon photoactivation of the highly reactive 1,6-DHP moiety, followed by a stepwise pathway to furnish the *iboga*-type product **5**. Moreover, we were able to harness the biradical excited state of the DHP moiety, together with appropriate conformational pre-organisation, to generate two novel *unnatural* scaffolds **8** and **9** *via* divergent [2 + 2] cycloadditions, including construction of a pentacyclic spiroindoline-type product *via* the dearomatisation of the indole ring. Simple modification of the substituent at the vinyl indole position allowed precise control of both the mode-of-cyclisation and diastereoselectivity, enabling divergent assembly of a total of three distinct indole alkaloidal fused scaffolds. We believe that the reactive 1,6-DHP ring, capable of undergoing thermal and photo-mediate transformations, holds untapped synthetic potential as a versatile intermediate to feasibly construct difficult-to-access molecular frameworks.

Data availability

The ESI† includes all experimental details, including optimisation of photoreaction conditions, synthesis and characterisation of compounds reported in this study, and mechanistic studies. Crystallographic data for **5h**, **8n**, and **9n** have been deposited under CCDC accession numbers 2333565, 2375152, and 2375172, respectively. The NMR spectra of all products, UV-vis spectra, crystallographic data, and computational modelling details are also included.

Author contributions

G. T. and S. N. contributed equally to this work. G. T., S. N., and H. O. conceived the projects and analysed the experimental results. G. T. and H. O. wrote the manuscript with feedback from S. N.

Conflicts of interest

A patent application for these photo-mediated divergent cyclisations of the multipotent intermediates will be filed by The University of Tokyo.

Acknowledgements

The authors thank Dr Haruki Mizoguchi, Hiroki Kubota, and Shun Oyadomari for preliminary synthetic investigations. We also appreciate Prof. Masanobu Uchiyama for discussions regarding radical trapping experiments. This work was supported in part by JSPS KAKENHI (JP19H02847, JP22H00346, and JP22H05127), the Naito Foundation, and the Asahi Glass Foundation (H. O.). G. Tay is grateful to the Global Science Graduate Course (GSGC) supported by The University of Tokyo. This work was also inspired by the international and interdisciplinary environments of the JSPS Asian CORE Program, "Asian Chemical Biology Initiative" as well as the JSPS A3 Foresight Program.

References

1 For selected papers, see: (*a*) R. D. Taylor, M. MacCoss and A. D. G. Lawson, *J. Med. Chem.*, 2014, **57**, 5845–5859; (*b*) E. K. Davison and J. Sperry, *J. Nat. Prod.*, 2017, **80**, 3060–3079; (*c*) C. Zhao, Z. Ye, Z. Ma, S. A. Wildman, S. A. Blaszczyk, L. Hu, I. A. Guizei and W. Tang, *Nat. Commun.*, 2019, **10**, 4015; (*d*) Y. Chen, C. Rosenkranz, S. Hirte and J. Kirchmair, *Nat. Prod. Rep.*, 2022, **39**, 1544–1556.

2 For selected papers, see: (*a*) K. Takao, R. Munakata and K. Tadano, *Chem. Rev.*, 2005, **105**, 4779–4807; (*b*) K. C. Nicolaou, S. A. Snyder, T. Montagnon and G. Vassilikogiannakis, *Angew. Chem., Int. Ed.*, 2002, **41**, 1668–1698; (*c*) A. A. Sara, U. Um-e-Farwa, A. Saeed and M. Kalesse, *Synthesis*, 2022, **54**, 975–998.

3 (*a*) R. B. Woodward and R. Hoffmann, *J. Am. Chem. Soc.*, 1965, **87**, 395–397; (*b*) R. B. Woodward and R. Hoffmann, *Angew Chem. Int. Ed. Engl.*, 1969, **8**, 781–932.

4 For selected papers, see: (*a*) N. Hoffmann, *Chem. Rev.*, 2008, **108**, 1052–1103; (*b*) B. Beeler, *Chem. Rev.*, 2016, **116**, 9629–9630.

5 For selected papers, see: (*a*) S. Poplata, A. Tröster, Y.-Q. Zou and T. Bach, *Chem. Rev.*, 2016, **116**, 9748–9815; (*b*) D. Sarkar, N. Bera and S. Ghosh, *Eur. J. Org Chem.*, 2020, **2020**, 1310–1326.

6 For selected papers, see: (*a*) J. Iriondo-Alberdi and M. F. Greaney, *Eur. J. Org. Chem.*, 2007, 4801–4815; (*b*) M. D. Kärkäs, J. A. Porco Jr and C. R. J. Stephenson, *Chem. Rev.*, 2016, **116**, 9683–9747.

7 For selected papers, see: (*a*) J. Sauer and R. Sustmann, *Angew Chem. Int. Ed. Engl.*, 1980, **19**, 779–807; (*b*) S. Jones and J. C. C. Atherton, *Tetrahedron: Asymmetry*, 2001, **12**, 1117–1119; (*c*) J. C. C. Atherton and S. Jones, *Tetrahedron*, 2003, **59**, 9039–9057.

8 For selected papers, see: (*a*) P. Wessig, A. Matthes and C. Pick, *Org. Biomol. Chem.*, 2011, **9**, 7599–7605; (*b*) J. Zhuang, S. Zhang, H. Hao and L. Jiang, *J. Photochem. Photobiol., A*, 2013, **270**, 14–18; (*c*) P. Wessig, D. Badetko and M. Koebe, *ChemistrySelect*, 2022, **7**, e202202648.

9 For selected papers, see: (*a*) B. Harirchian and N. L. Bauld, *J. Am. Chem. Soc.*, 1989, **111**, 1826–1828; (*b*) A. Gieseler,

E. Steckhan, O. Wiest and F. Knoch, *J. Org. Chem.*, 1991, **56**, 1405–1411; (*c*) M. Martiny, E. Steckhan and T. Esch, *Chem. Ber.*, 1993, **126**, 1671–1682; (*d*) M. A. Miranda and H. García, *Chem. Rev.*, 1994, **94**, 1063–1089; (*e*) J. Pérez-Prieto, S. E. Stiriba, M. González-Béjar, L. R. Domingo and M. A. Miranda, *Org. Lett.*, 2004, **6**, 3905–3908; (*f*) M. González-Béjar, S. E. Stiriba, L. R. Domingo, J. Pérez-Prieto and M. A. Miranda, *J. Org. Chem.*, 2006, **71**, 6932–6941; (*g*) S. Lin, M. A. Ischay, C. G. Fry and T. P. Yoon, *J. Am. Chem. Soc.*, 2011, **133**, 19350–19353; (*h*) S. Lin, C. E. Padilla, M. A. Ischay and T. P. Yoon, *Tetrahedron Lett.*, 2012, **53**, 3073–3076; (*i*) S. P. Pitre, J. C. Scaiano and T. P. Yoon, *ACS Catal.*, 2017, **7**, 6440–6444; (*j*) K. Nakayama, N. Maeta, G. Horiguchi, H. Kamiya and Y. Okada, *Org. Lett.*, 2019, **21**, 2246–2250.

10 For selected papers, see: (*a*) J. Ma, S. Chen, P. Bellotti, R. Guo, F. Schäfer, A. Heusler, X. Zhang, C. Daniliuc, M. K. Brown, K. N. Houk and F. Glorius, *Science*, 2021, **371**, 1338–1345; (*b*) P. Rai, K. Maji, S. K. Jana and B. Maji, *Chem. Sci.*, 2022, **13**, 12503–12510; (*c*) R. Guo, S. Adak, P. Bellotti, X. Gao, W. W. Smith, S. N. Le, J. Ma, K. N. Houk, F. Glorius, S. Chen and M. K. Brown, *J. Am. Chem. Soc.*, 2022, **144**, 17680–17691.

11 G. Quinkert, W.-D. Weber, U. Schwartz and G. Dürner, *Angew Chem. Int. Ed. Engl.*, 1980, **19**, 1027–1029.

12 K. C. Nicolaou, D. Gray and J. Tae, *Angew. Chem., Int. Ed.*, 2001, **40**, 3675–3678.

13 N. C. Yang and C. Rivas, *J. Am. Chem. Soc.*, 1961, **83**, 2213.

14 J. L. Sugura and N. Martín, *Chem. Rev.*, 1999, **99**, 3199–3246.

15 For selected papers, see: (*a*) R. N. Iyer, D. Favela, G. Zhang and D. E. Olsen, *Nat. Prod. Rep.*, 2021, **38**, 307–329; (*b*) B. M. M. Michele and A. A. Sophie, *Pharmacol. Res. Nat. Prod.*, 2023, **1**, 100006.

16 H. Mizoguchi, H. Oikawa and H. Oguri, *Nat. Chem.*, 2014, **6**, 57–64.

17 H. Mizoguchi, R. Watanabe, S. Minami, H. Oikawa and H. Oguri, *Org. Biomol. Chem.*, 2015, **13**, 5955–5963.

18 For selected papers, see: (*a*) T. H. Rehm, *Chem. Eur. J.*, 2020, **26**, 16952–16974; (*b*) T. Fukuyama, T. Kasakado, M. Hyodo and I. Ryu, *Photochem. Photobiol. Sci.*, 2022, **21**, 761–775; (*c*) L. Buglioni, F. Raymenants, A. Slattery, S. D. A. Zondag and T. Noël, *Chem. Rev.*, 2022, **122**, 2752–2906; (*d*) S. D. A. Zondag, D. Mazzarella and T. Noël, *Annu. Rev. Chem. Biomol. Eng.*, 2023, **14**, 283–300; (*e*) A. Slattery, Z. Wen, P. Tenblad, J. S. J. Orduna, D. Pintossi, T. D. Hartog and T. Noël, *Science*, 2024, **383**, 382.

19 Crystallographic data for **5h**, **8n**, and **9n** have been deposited under accession numbers 2333565, 2375152, and 2375172, respectively.

20 E. B. McLean, F. M. Cutolo, O. J. Cassidy, D. J. Burns and A.-L. Lee, *Org. Lett.*, 2020, **22**, 6977–6981.

21 For selected papers, see: (*a*) M. Zhu, C. Zheng, X. Zhang and S.-L. You, *J. Am. Chem. Soc.*, 2019, **141**, 2636–2644; (*b*) Z. Zhang, D. Yi, M. Zhang, J. Wei, J. Lu, L. Yang, J. Wang, N. Hao, X. Pan, S. Zhang, S. Wei and Q. Fu, *ACS Catal.*, 2020, **10**, 10149–10156; (*c*) M. Zhu, X. Zhang, C. Zheng and S.-L. You, *Acc. Chem. Res.*, 2022, **55**, 2510–2525.

22 G. Tay, T. Wayama, H. Takezawa, S. Yoshida, S. Sato, M. Fujita and H. Oguri, *Angew. Chem., Int. Ed.*, 2023, **62**, e202305122.

23 (*a*) B. J. Deppmeier, A. J. Driessen, W. J. Hehre, T. S. Hehre, J. A. Johnson, S. Ohlinger and P. E. Klunzinger, *Spartan 20*, Wavefunction Inc., Irvine CA, 2020; (*b*) Y. Shao, *et al.*, *Mol. Phys.*, 2015, **113**, 184–215.

24 For selected papers, see: (*a*) G. E. M. Crisenza, D. Mazzarella and P. Melchiorre, *J. Am. Chem. Soc.*, 2020, **142**, 5461–5476; (*b*) Y. Yuan, S. Majumder, M. Yang and S. Guo, *Tetrahedron Lett.*, 2020, **61**, 151506.

25 T. Wayama, Y. Arai and H. Oguri, *J. Org. Chem.*, 2022, **87**, 5938–5951.

26 For selected papers, see: (*a*) Y. Li, Y. Hu, S. Zhang, J. Sun, L. Li, Z. Zha and Z. Wang, *J. Org. Chem.*, 2016, **81**, 2993–2999; (*b*) S. Reymond and J. Cossy, *Chem. Rev.*, 2008, **108**, 5359–5406.

27 For selected papers, see: (*a*) F. W. Fowler, *J. Org. Chem.*, 1972, **37**, 1321–1323; (*b*) P. Beeken, J. N. Bonfiglio, I. Hasan, J. J. Piwinski, B. Weinstein, K. A. Zollo and F. W. Fowler, *J. Am. Chem. Soc.*, 1979, **101**, 6677–6682; (*c*) S. M. N. Sieburth, *CRC Handbook of Organic Photochemistry and Photobiology*, CRC Press, 2004, 2nd edn, p. 103; (*d*) S. C. Coote, *Eur. J. Org Chem.*, 2020, 1405–1423.